SHORT COMMUNICATION

Structural differentiation of the mesozooplankton community in two hydrographic domains of a small basin: the frontal system of San José Gulf (Patagonia, Argentina) as a study case

RODRIGO D. HERNÁNDEZ MORESINO[1]*, LUJAN VILLANUEVA GOMILA[1], ROXANA DI MAURO[2] AND PEDRO J. BARÓN[1,3]

[1]CENTRO NACIONAL PATAGÓNICO (CENPAT), CONSEJO NACIONAL DE INVESTIGACIÓN CIENTÍFICAS Y TÉCNICAS (CONICET), BOULEVARD BROWN 2915 (U9120ACD), PUERTO MADRYN, ARGENTINA, [2]DEPARTMENT OF OCEANOGRAPHY AND COASTAL SCIENCES, LOUISIANA STATE UNIVERSITY, BATON ROUGE, LA, USA AND [3]FACULTAD REGIONAL CHUBUT − UNIVERSIDAD TECNOLÓGICA NACIONAL, PUERTO MADRYN, CHUBUT, ARGENTINA

*CORRESPONDING AUTHOR: rodrigo@cenpat.edu.ar

The structure of the mesozooplankton community of San José Gulf, Argentina, was analyzed in two hydrographic domains developed during the formation of a spring−summer frontal system. Abundance peaked in December in both domains, remaining high in February only in the stratified east domain (ED). Copepods were the most abundant taxon, with larger individuals in the vertically mixed west domain (WD). Overall, larger individuals (large copepods) dominated the WD, while smaller individuals (small copepods and cladocerans) prevailed in the ED.

San José Gulf (SJG) is a shallow and semi-enclosed basin (surface area: 817 km^2; mean depth: 40 m) that opens to the north into the much larger and deeper San Matías Gulf (SMG) (surface area: 18 000 km^2, mean depth: 100 m) through a narrow (6.9 km) mouth (Rivas, 1990) (Fig. 1A). High levels of nutrients and primary productivity in its waters, similar to those reported for upwelling areas, have been attributed to the entrance of nutrient-rich water masses from adjacent areas (Charpy *et al.*, 1980; Esteves *et al.*, 1986). This highly productive watershed provides trophic support to a small-scale fishery operating on the Tehuelche scallop (*Aequipecten tehuelchus*) (Orensanz *et al.*, 2007), which has constituted most of the regional shellfish production for more than three decades (Amoroso *et al.*, 2011).

Recently, the analysis of high-resolution satellite images allowed the identification of a longitudinal surface frontal system in SJG, dividing it into two well-defined hydrographic (west and east) domains (Amoroso and Gagliardini, 2010). The hydrodynamics of the west domain (WD) is strongly influenced by tidal currents circulating through the mouth, whereas that of the east domain (ED) is not significantly affected by tidal circulation. Consequently, vertical mixing induced by advective fluxes in the WD prevents stratification year-round, whereas low renewal rate in the ED allows the evolution of a well-marked thermocline from late spring to summer (Crespi-Abril *et al.*, 2013). Moreover, satellite images

confirm previous suggestions that nutrient-rich waters from the Valdés Peninsula tidal front (Carreto *et al.*, 1995) are transported into SJG through its mouth (Fig. 1B).

Since structural differences in zooplankton communities have been found on opposite sides of several marine frontal systems (Sabatini and Martos, 2002; Alcaraz *et al.*, 2007), it is likely that both domains of SJG differ in the mesozooplankton community structure (abundance and composition of taxa) associated with their particular hydrographic conditions. Indeed, differences in the spatial distribution of the most abundant bivalve species with meroplanktonic larvae support this hypothesis: while Tehuelche scallops aggregate in the ED (Amoroso *et al.*, 2011), the mussels *Aulacomya atra atra* and *Mytilus edulis platensis* are found in the WD (Zaixso, 2004). However, no study has focused on the structure of the zooplankton community in SJG and the potential link between it and the prevailing hydrodynamic conditions.

The development of semi-automated zooplankton counting and classification methods provides new options for the study of plankton communities (Benfield *et al.*, 2007; Grosjean and Denis, 2007). Image analysis allows the processing of a higher number of samples than under-microscope classification, with less effort and time but offering lower taxonomical resolution. Based on the use of this technique, we tested if there are differences in the structure of the mesozooplankton community
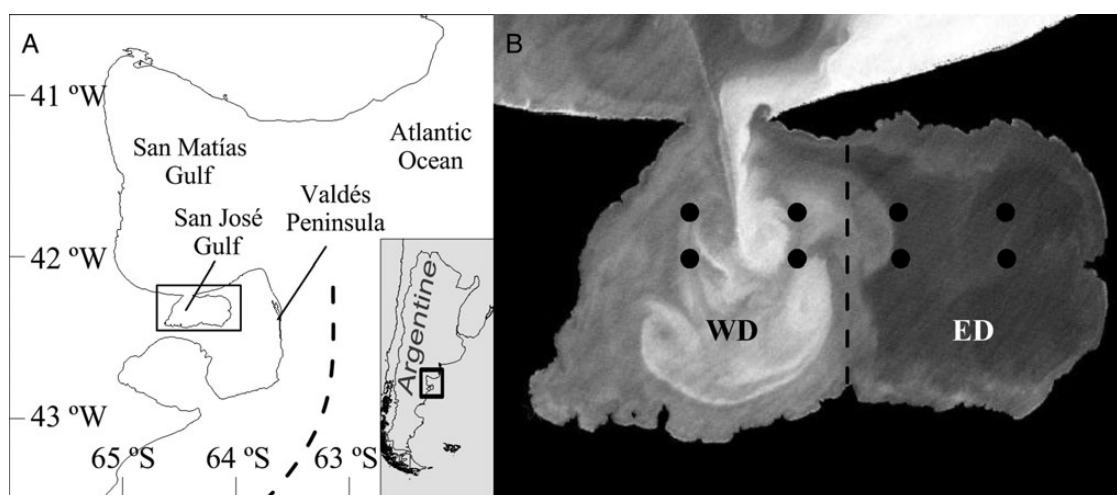

Fig. 1. Study area (**A**). Landsat image illustrating the distribution of suspended sediments in the surface of San José Gulf (lighter tones correspond to higher sediment concentration). Image provided by R. A. Amoroso and D. A. Gagliardini (**B**). Broken lines indicate the location of the frontal systems: curve line (in A) indicates tidal front of Valdés Peninsula and straight line (in B) indicates SJG front. WD and ED denote the west and east domains, respectively. Circles (in B) indicate the location of sampling stations.

between both domains of SJG that could be related to their contrasting hydrographic conditions.

Sampling was conducted on a nearly monthly basis from October 2011 to March 2012 using a fixed grid including four stations on each side of the frontal system of SJG (Fig. 1B). At each, a Hensen net (0.7-m diameter and 295-μm mesh) with a mechanical flowmeter (General Oceanic, model R 2030) attached to its mouth was towed from bottom to surface at ~ 1 m s^{-1}. Rough weather prevented sampling on January 2012 and at some stations in the remaining months; thus a total of 32 samples were obtained and stored in 5% formalin for further analysis.

Aliquots of 4% the volume of the original samples were stained with Bengal Rose for 24 h to ensure good contrast. Then, they were digitized with a Canon Powershot D10 12.1 Mp camera mounted on a mechanical arm to keep the distance above the camera and the field of depth constant for all images (i.e., 14 cm and f/2.8, respectively). Polystyrene cel006Cs (10 × 10 cm) were used to place small portions of the aliquots and a uniform background light was created by placing a diffusive layer between the light source and the cell. As a result, 452 raw images (1529 ppi resolution, 24 bit color) were obtained with previous calibration of pixel size to 0.0166×0.0166 mm^2.

Images were processed using ZooImage version 1.2-1 (http://www.sciviews.org/zooimage) to automatically count and identify the organisms (Grosjean and Denis, 2007). To estimate abundance (ind. m^{-3}), the software relied on a training set in which part of the extracted vignettes (individual snapshots of the organisms) were included in three non-biological categories that were not used further in the analysis (in the total abundance estimations) and eight biological categories. The training set was combined with the random forest learning algorithm to create the classifier. This is the statistical representation of the training set that constitutes a multivariate reference in which all vignettes extracted from the samples are compared and eventually classified in the most similar category.

The performance of the ZooImage classifier was assessed by calculating a k-fold cross-validation matrix that constitutes the visual tool to assess the accuracy (%) of the classifier. The k-fold cross-validation process entails the random partitioning of the training set into k parts (folds) and the classifier is created and evaluated k times, each time using a different part. By default, ZooImage uses $k = 10$ and the overall error reported at the end of the analysis corresponds to the average error of the trials. This confusion matrix not only allows the identification of the wrongly classified vignettes but also categories from which these originate. Finally, to generate more accurate estimates of abundance, results for each

category were corrected by using the coefficients (CC = visual inspection/ZooImage classification) estimated in the confusion matrix.

A multifactorial ANOVA was conducted using Statistica 7.0 (StatSoft Inc.) to evaluate differences in abundance and body size between domains and months. Body size was also provided by ZooImage as equivalent circular diameter (ECD), which constitutes the most accurate variable that can be obtained automatically to represent size (Di Mauro et al., 2011). The data were log-transformed to obtain normalized frequency distribution of each sample. In the case of abundance data, log-transformation was applied as $\log_{10}(x + 1)$ to avoid difficulty with zero values. When the results of the ANOVA test were significant, pair-dependent sample comparisons were performed using the Tukey HSD test (Zar, 1999).

The final training set, including 11 categories, presented the lowest error obtained after several preliminary tests of merge/separate categories with a general estimated accuracy of 84.25% (Table I).

Differences in mesozooplankton abundance were found in the interaction between domains and months $(F_{(4,22)} = 27.89, P < 0.01)$ (Fig. 2A). The Tukey HSD test revealed that highest abundances occurred in December in both domains and were still high in February only in the ED. Thus, differences between domains were evident only in February when abundance remained higher in the ED and decreased in the WD. These differences were high enough to indicate that the ED's water column has a higher average abundance than the WD $(F_{(1,22)} = 14.56, P < 0.01)$.

To clarify the particular contribution of each taxon to the total abundance, values were calculated separately (data not shown). All taxa showed differences in abundance through the time series $(F_{(4,22)}, P < 0.01)$, with high values in December in the WD and in December and February in the ED. Fish larvae were the exception, showing significantly higher abundance only in the ED in February. Differences in abundance between domains were also observed, but only for Cladocera, fish larvae, fish eggs (grouping egg-elongated and egg-round categories) and Appendicularia-Chaetognatha $(F_{(1,22)}, P < 0.01)$. In cases where differences between domains were evident, the average values in the ED were higher than those in the WD.

Overall, Copepoda contributed with 68,6% of the total mesozooplankton abundance, followed by Cladocera, Malacostraca larvae, Malacostraca adults, fish eggs, Appendicularia-Chaetognatha and fish larvae (16.3, 7.3, 4.2, 1.8, 1.7 and 0.1%, respectively). Most of the zooplankton community was produced in pulses occurring in both domains in December and in the ED in February, representing 98.4% of the total abundance.

Table I: Confusion matrix obtained for the training set after classification with random forest algorithm

General accuracy (%) 84.25	ZooImage classification prediction											CC
	1	2	3	4	5	6	7	8	9	10	11	
User classification in training set												
Appendicularia-Chaetognatha (1)	102	1	0	0	3	0	0	1	4	2	0	1.16
Badimages-Shadows (2)	7	261	23	23	15	2	1	7	1	6	9	1.00
Bubbles (3)	0	6	53	2	0	0	0	0	0	0	0	1.31
Cladocera (4)	0	44	3	545	5	0	3	1	0	19	0	0.95
Copepoda (5)	6	14	0	1	524	0	0	3	22	41	0	0.97
Egg, elongated (6)	0	1	0	2	0	126	2	0	0	0	0	0.99
Egg round (7)	0	4	1	0	0	1	275	0	0	1	0	0.98
Fish larvae (8)	1	6	0	0	3	0	0	175	0	4	1	1.01
Malacostraca adult (9)	11	2	0	0	17	0	0	1	254	44	0	1.04
Malacostraca larvae (10)	4	15	0	16	25	1	0	3	62	347	0	0.98
Scrachs-fibers (11)	0	1	0	0	0	0	0	0	0	0	34	1.26
Total	131	355	80	589	592	130	281	191	343	464	44	
Accuracy (%)	77.9	73.5	66.3	92.5	88.5	96.9	97.9	91.6	74.1	74.8	77.3	

Rows represent the groups in the training set labeled by the user, whereas columns (1–11, same categories as rows) show the classification by ZooImage. Numbers in the diagonal line (in grey) represent the correct classification of vignettes (true positives), while those outside correspond to misclassified individuals (false positives). CC denotes the correction coefficient used to generate more accurate estimations of abundance.
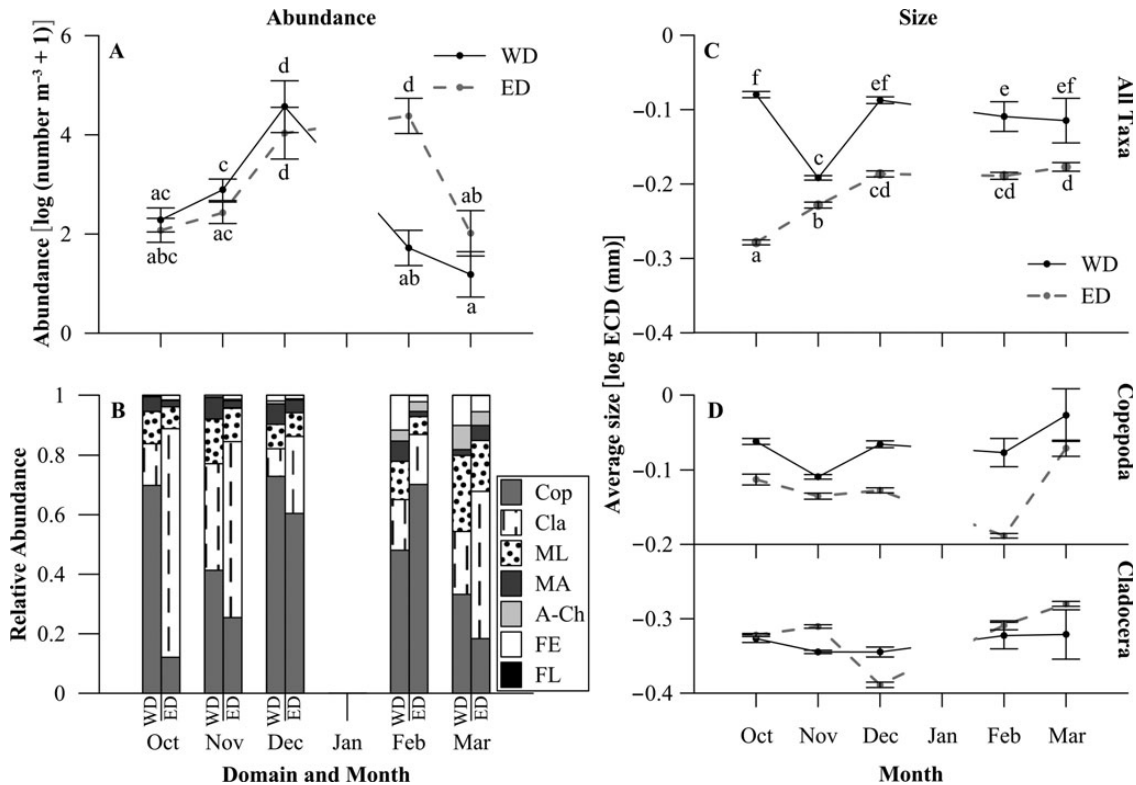

Fig. 2. Abundance (**A** and **B**) and body size (**C** and **D**) plots of mesozooplankton in the two hydrographic domains during the sampling period. Absolute and relative abundance is shown in (A) and (B), respectively. Average size distribution was plotted grouping all taxa (C) and for Copepoda and Cladocera (D). Circles in (A), (C) and (D) represent log-transformed average data and error bars indicate 95% confidence intervals. Each lower case letter on top and bottom of the error bars indicate an homogeneous group from the Tukey HSD test. WD and ED denote the West and East domains, respectively. Co, Copepoda; Cla, Cladocera; ML, Malacostraca larvae; MA, Malacostraca adult; A-Ch: Appendicularia-Chaetognatha; FE, fish eggs; FL, fish larvae.

Copepoda was also the most abundant taxon in 7 out of the 10 grouping cases (i.e. combinations of domain and month cases, Fig. 2B), encompassing 72.1 and 66.3% of

the total abundance in the WD and the ED, respectively. The remaining three cases, all from the ED, were dominated by Cladocera, encompassing 10 and 20.4% of the

total abundance in the WD and the ED, respectively. Except for February, Copepoda were more frequent in the WD than in the ED and Cladocera were more frequent in the ED in all months sampled (Fig. 2B).

Visual inspection of the raw images revealed other interesting results. Almost all copepods ($>90\%$) were calanoids in both domains and all months. Two groups of calanoids stood out; one of large Calanidae (body length >1.5 mm) accounting for 34% of the abundance (44% in the WD and 23% in the ED), and the other including a variety of small calanoids (body length <1.5 mm) forming 66% of the abundance (56% in the WD and 76% in the ED). For cladocerans, a sequential species replacement was observed, shifting from dominance of *Evadne nordmanni* during the first 3 months ($>80\%$) to that of *Podon* spp. in the last 2 months, when *E. normanni* was virtually absent. In the case of Appendicularia-Chaetognatha, the group was mainly represented by chaetognaths (ca. 88%). Finally, almost all malacostracans belonged to Decapoda and Mysidacea.

Size structure was also analyzed based on the average log-transformed ECD. Differences in the interaction between domains and months were observed when grouping all the taxa ($F_{(4,50339)} = 420.56$, $P < 0.01$, Fig. 2C). Overall, the vertically mixed domain (WD) showed larger organisms than the vertically stratified one (ED) ($F_{(1,50339)} = 731.02$, $P < 0.01$). Size in the WD was almost constant though the time series, except for November when average size showed a minimum value probably due to the high abundance of small-sized cladocerans (Fig. 2B). In contrast, the ED increased continuously in the average size through the time series.

Of all the taxa, only Copepoda and Cladocera showed clear differences in the size structure between domains. Copepods were larger in the WD ($F_{(1,23393)} = 182.24$, $P < 0.01$), while cladocerans were larger in the ED ($F_{(1,18817)} = 9.52$, $P < 0.01$). Marked reductions in the average size were observed in the ED for Copepoda in February and for Cladocera in December (Fig. 2D).

Two major results arise from this study: (i) hydrographic domains in the SJG display clear differences in their mesozooplankton total abundance, size structure and relative frequency of major taxa and (ii) peaks of mesozooplankton occur in December in both domains, but occur only in the ED (vertical stratified) in February.

Differences in the total abundance between domains are associated only with some of the taxa. Copepods, for example, show no clear preference for any domain, shifting in maximum abundance from one domain to the other through the time series. This pattern was expected, since most of the copepods found in our samples were Calanoid, and Sabatini and Martos (2002) reported that these are abundant over the whole frontal system off

Valdés Peninsula. However, it is worth noting that the mesh size of the net we used was rather coarse (295 μm), probably resulting in the underestimation of the smallest-sized mesozooplankton fraction including oithonids, which frequently represent a higher percentage of the total abundance. Although cladocerans were present in high numbers in both domains of SJG, they were more frequent in the ED suggesting that stratified waters are more favorable. Likewise, species from this group peak in poorly stratified transitional waters of the frontal system off Valdés Peninsula, being less abundant in highly mixed waters (Sabatini and Martos, 2002; Viñas *et al.*, 2007). Seasonal succession observed here in species from this group (i.e. replacement of *Evadne nordmanni* by the larger *Podon* spp.) has been previously observed in freshwater environments, where a size-dependent pattern of small-bodied species shifting to larger ones in early summer was related to size-selective predation, resource limitation and/or interspecific competition (Dohet and Hoffmann, 1995).

Apart from copepods and cladocerans, mesozooplankton abundance in SJG is dominated by Malacostraca (adults and larvae) and Appendicularia-Chaetognatha, the former being equally distributed between domains and the latter being more frequent in the WD. It is worth mentioning that the dominance of chaetognaths (ca. 88%) over appendicularians (ca. 12%) contrasts with the results of studies conducted in the Valdés Peninsula frontal system, in which appendicularians occur at higher concentrations in comparison with chaetognaths (Sabatini and Martos, 2002; Capitanio *et al.*, 2005). However, as in the case of oithonids, it should be mentioned that abundance of small appendicularians could have been underestimated due to the coarse mesh we used.

A chronological comparison of the relative frequency of major taxa between domains (Fig. 2B) reveals that copepods and cladocerans, respectively, dominate the WD and ED in most months. This could be the reason why the WD shows larger mesozooplankton than the ED (Fig. 2C). Differences in mesozooplankton size spectra between domains may be related to the size of available food. It is well known that well mixed, rich nutrient waters usually support large cells and large copepods, while small cells and protozooplankton prevail in stratified nutrient-poor waters where small copepods are regularly more abundant (Le Fèvre, 1987). However, this would not explain the dominance of larger cladocerans in the ED (Fig. 2D).

It is interesting to note that there is a continuous increase in the average size structure in the ED throughout the time series that is not observed in the WD, where the size structure stays almost constant (Fig. 2C). To explain these differences, it should be considered that as the formation of the frontal system progresses, nutrients available for primary production probably became exhausted

in the upper layer of the ED, but stay more or less constant and at high levels in the permanently well-mixed WD. Therefore, the more constant food supply conditions at the WD should be reflected in a nearly constant structure of the trophic levels and of the mesozooplankters within them. In contrast, as nutrient availability reduces in the ED, a species/ontogenic-stage succession must occur, starting from high abundance of smaller early life stages and phytoplankton grazers at the beginning of the season (when primary productivity is at its highest level), followed by the dominance of older (larger) ontogenic stages and also larger species from upper trophic levels.

The high mesozooplankton abundance in February in the ED could be explained by hydrographic characteristics of SJG. Regarding this, a mechanism was proposed by Crespi-Abril *et al.* (Crespi-Abril *et al.*, 2013), who suggested that the front between domains may act as a retention area, concentrating part of mesozooplankton carried by tidal currents to the WD in its boundary and delivering them to the ED where circulation is low.

Summarizing, high mesozooplankton production in SJG peaking in December and February seems to be the result of the seasonal development of the frontal system and the advection of nutrients, phytoplankton and zooplankton from the Valdés Peninsula fontal area. Clearly, our results are insufficient to test all potential explanations for the differences between domains but do shed light on the contrasting structure of the mesozooplankton community (i.e. abundance, size spectra and relative taxa composition) of the two water masses. Further sampling must be conducted including day−night stratified tows and extending the sampling period to evaluate year-round patterns.

REFERENCES

Alcaraz, M., Calbet, A., Estrada, M. *et al.* (2007) Physical control of zooplankton communities in the Catalan Sea. *Prog. Oceanogr.*, **74**, 294−312.

Amoroso, R. O. and Gagliardini, D. A. (2010) Inferring complex hydrographic processes using remote-sensed images: turbulent fluxes in the Patagonian Gulfs and implications for scallop metapopulation dynamics. *J. Coast. Res.*, **26**, 320−332.

Amoroso, R. O., Parma, A. M., Orensanz, J. M. *et al.* (2011) Zooming the macroscope: medium-resolution remote sensing as a framework for the assessment of a small-scale fishery. *ICES J. Mar. Sci.*, **68**, 696−706.

Benfield, M. C., Grosjean, P., Culverhouse, P. F. *et al.* (2007) RAPID: research on automated plankton identification. *Oceanography*, **20**, 172−187.

Capitanio, F. L., Pájaro, M. and Esnal, G. B. (2005) Appendicularians: an important food supply for the Argentine anchovy *Engraulis anchoita* in coastal waters. *J. Appl. Ichthyol.*, **21**, 414−419.

Carreto, J. I., Lutz, V. A., Carignan, M. O. *et al.* (1995) Hydrography and chlorophyll a in a transect from the coast to the shelf-break in the Argentinian Sea. *Cont. Shelf Res.*, **15**, 315−336.

Charpy, L. J., Charpy-Roubaud, C. J. and Pizarro, M. J. (1980) La production primaire des eaux du Golfe San Jos (Peninsule Valdes, Argentine). I. Parametres physiques et teneurs en sels mineraux. *Hydrobiologia*, **75**, 209−214.

Crespi-Abril, A. C., Villanueva Gomila, L., Venerus, L. A. *et al.* (2013) Spatial distribution of cephalopod paralarvae in San José Gulf (Northern Patagonia, Argentina): the role of tidal circulation in larval dispersal. *Fish. Res.* doi:10.1016/j.fishres.2013.07.002.

Di Mauro, R., Cepeda, G., Capitanio, F. *et al.* (2011) Using ZooImage automated system for the estimation of biovolume of copepods from the northern Argentine Sea. *J. Sea Res.*, **66**, 69−75.

Dohet, A. and Hoffmann, L. (1995) Seasonal succession and spatial distribution of the zooplankton community in the reservoir of Esch-sur-Sûre (Luxembourg). *Belg. J. Zool.*, **125**, 109−123.

Esteves, J. L., Solis, M., Cejas, J. *et al.* (1986) Golfo San José: Resultados de las campañas oceanográficas 1984/1985. Report to the Chubut Province Administration. CENPAT, Puerto Madryn, Argentina, p. 13.

Grosjean, P. and Denis, K. (2007) ZooImage users manual. www. sciviews.org/zooimage.

Le Fèvre, J. (1987) Aspects of the biology of frontal systems. In Blaxter, J. H. S. and Southward, A. J. (eds), *Adv. Mar. Biol*, Vol. 23. Academic Press, London, pp. 163−299.

Orensanz, J. M., Parma, A. M., Ciocco, N. *et al.* (2007) Achievements and setbacks in the commercial diving fishery of San José Gulf, Argentine Patagonia. In McClanahan, T. R. and Castilla, J. C. (eds), *Fisheries Management: Progress Towards Sustainability.* Blackwell Publishing Ltd, Oxford, pp. 68−87.

Rivas, A. (1990) Heat balance and annual variation of mean temperature in the North-Patagonian gulfs. *Oceanol. Acta*, **13**, 265−272.

584

Sabatini, M. E. and Martos, P. (2002) Mesozooplankton features in a frontal area off northern Patagonia (Argentina) during spring 1995 and 1998. *Sci. Mar.*, **66**, 215–232.

Viñas, M., Ramírez, F. C., Santos, B. *et al*. (2007) Spatial and temporal distribution patterns of Cladocera in the Argentine Sea. *Hydrobiologia*, **594**, 59–68.

Zaixso, H. E. (2004) Bancos de cholga *Aulacomya atra atra* (Molina) (Bivalvia: Mytilidae) del golfo San José (Chubut, Argentina): Diversidad y relaciones con facies afines. *Rev. Biol. Mar. Oceanogr.*, **39**, 61–78.

Zar, J. H. (1999) Biostatistical Analysis, *4th edn*. Prentice Hall, New Jersey.